

# POLITECNICO DI TORINO

## *Master's degree in Mechanical Engineering*

Mechanical, Aerospace, Automotive and Production Engineering Department



## *Data analysis of a scale vehicle shock absorber*

### **Supervisors:**

*Vigliani Alessandro*  
*Bonisoli Elvio*  
*Vella Domenico Angelo*  
*Lisitano Domenico*

### **Candidate:**

*Samuel Pagliari*

*Torino, 16 Dicembre 2021*

# Index

Index.....	2
Abstract .....	3
Introduction.....	4
1. Experimental testing .....	5
1.1 Shock absorber.....	7
2. Preliminary analysis.....	9
2.1 Force and displacement signals analysis.....	10
2.2 Velocity and acceleration.....	15
2.3 Experimental damping force.....	17
2.4 Interpolation of the damping force.....	21
2.4.1 Damping coefficients and interpolation error .....	22
3. Frequency effect on damping coefficients .....	24
4. Comparison between front and rear .....	25
5. Comparison between different piston displacements.....	27
5.1 Damping coefficients for different displacements .....	29
6. Comparison between different oil viscosities .....	31
6.1 Damping coefficients for different viscosities .....	34
7. 3D maps of the damping coefficients .....	37
Conclusions.....	39
Reference .....	40

## **Abstract**

The aim is to analyze and postprocess the data, obtained through previous experimental tests done on shock absorbers of a 1:5 scale model car using oils of several viscosities and imposing different piston displacements, by creating a damping model that considers these data. It is therefore necessary to post-process the information to identify the non-linear characteristics of the shock absorbers. The preliminary analysis consists of examining only two tests with two oils of different viscosity at equal displacement to find the damping characteristic and see the main differences on a small scale. Then, the analysis extends to all other data, making considerations about comparisons between front and rear case at the same viscosity for different displacements and at the same displacement for different viscosities.

## **Introduction**

The objective of the thesis is to analyze the experimental measurements and data of a previous activity, concerning shock absorbers for a vehicle in 1:5 scale, and to create a damping model that considers these data, identifying a damping characteristic, function of displacement and viscosity.

It is known that an ideal damper is purely viscous but from the data provided this is not exactly the case because there are other factors to consider. It is therefore necessary to post-process the information obtained to be able to identify two main effects: both that of friction, which is a secondary effect but important for the non-linear characteristics of the shock absorber, and the fact that we have a viscous behavior that could be non-linearly dependent on speed.

For this thesis, a 1:5 scale vehicle was used because compared to a normal car it is a rather simple object. However, it has a considerable cost, as it has a very advanced dynamic model, i.e. a good suspension both front and rear, and has a very sophisticated adjustability, i.e. you can change both the elastic elements and the oil in the shock absorbers through which can change the feature. On a real vehicle it would be impossible to make such a study because the setup costs would be so high as to be comparable to those of a company that produces shock absorbers but not with a survey perspective of this type.

# 1. Experimental testing

Engineer De Giuseppe, the author of the previous thesis, was responsible for characterizing a highly variable element of this scale model with the aim of seeing the effect that the shock absorbers have on the complex behavior of the structure. The goal of his thesis was to characterize shock absorbers with experimental tests in terms of speed and displacement. The diagram below in Figure 1.1 was obtained with numerical simulations in a program called Lupos and was intended to be reproduced experimentally on a program called Losi 5ive. Therefore, if the framework of the vehicle in which the effect of the shock absorbers is changed is assumed, the objective of the experimental part was to obtain the continuous curves of the graph, which vary according to a parameter, and these curves should be followed in a continuous line. The black dots, if the undamped system is on the imaginary axis, represent the reference condition. So, the final objective of the activity was to discreetly derive these trends of the poles with various settings of springs and shock absorbers in the vehicle.

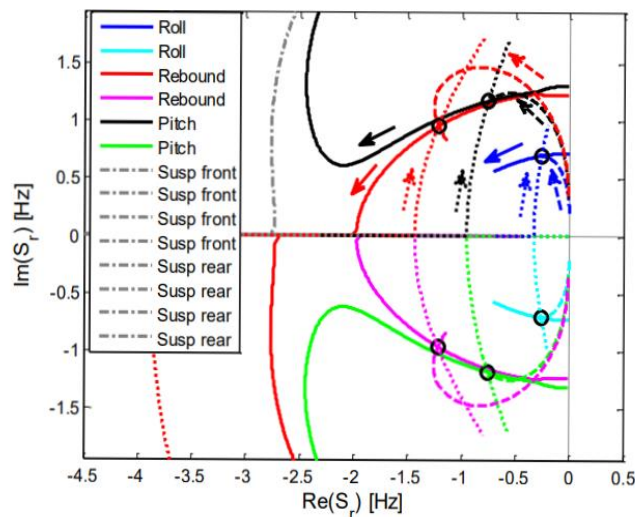


Figure 1.1 – Parametric Complex Modal Analysis of the damped system eigenvalues: detail of chassis body eigenvalues varying suspension damping (solid lines), tyre stiffness (dashed lines), suspension stiffness (dotted lines), nominal model has ball symbols [1].

The shock absorber setup is characterized by various elements: there is a shaker, the data acquisition system with the laser and the load cell, the plate where one of the two ends of the shock absorber is blocked and in the upper part a support which should be quite rigid to have a firm reference. What has been done is to characterize the dampers and apply a scheme in which the displacement of an extreme is defined with the shaker by making a frequency sweep (from  $f_1$  to  $f_2$  with assigned slope). The displacement is measured by a laser which gives feedback to the measurement system. On the other hand, we have a load cell that allows us to measure the force necessary to maintain this controlled law of the shaker and therefore we can acquire a characteristic as a function of the exciting frequency. So, in your Acquisition System you have the force and displacement signal at the input, the voltage that powers the shaker at the output.

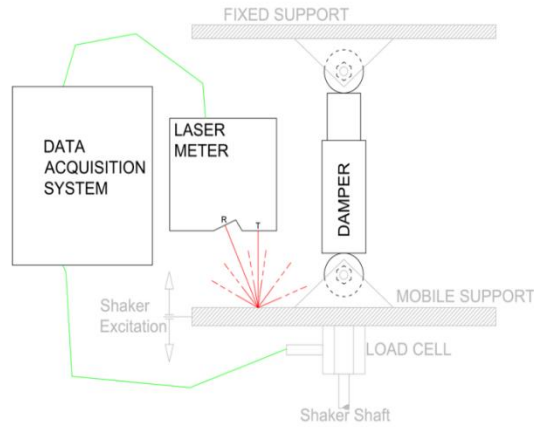


Figure 1.2 – Scheme of the damper experiment [1].

This test bench allowed to obtain some experimental data. The displacement is a sine wave and as it evolves over time the frequency is increasing, so a constant displacement frequency sweep is done (the magnitude of the imposed displacement is kept constant). Obviously, the speed will increase linearly, and the acceleration will be parabolic. The measured forces are therefore increasing as we increase the frequency, but in their dependence on the displacement and velocity they have a particular surface called "restitution" which depends on the velocity in viscous terms but is also dependent on the displacement and therefore we note for example the effect of friction (areas more pronounced for high displacements and when we reach the limits of the oscillation and therefore the Coulomb effects of static friction are predominant). So, it is not trivial to have an effective model from these data.

## 1.1 Shock absorber

A shock absorber or damper is a mechanical or hydraulic device designed to absorb and damp shock impulses. It does this by converting the kinetic energy of the shock into another form of energy (typically heat) which is then dissipated. Most shock absorbers are a form of dashpot (a damper which resists motion via viscous friction), like in this case [2].

The shock absorber mainly consists of a piston that is mounted on a stem and then inserted into a cylinder. Finally, a rubber cap covers the stem and prevents oil leaks.



Figure 1.1.1 – Shock absorber used for the tests [1].

As it was said this shock absorber was mounted on a RC car model that is shown in Figure 1.1.2.



Figure 1.1.2 – RC car model [1].

The cylinder is then filled with silicone oil of different viscosities, starting from WT20 up to WT100, for a total of 12 gradations.



Figure 1.1.2 – The 12 different oils [1].

Silicone is used for many different things, but the use of it in shock oil is because of its incredible lubricating properties. Keeping the parts of the vehicle that absorb the impacts of a crash lubricated prevents maximum damage to the parts. Silicone-based shock oil is better for the environment than the other options of motor oil, as well [3].

Other advantages of using silicone-based shock oil include:

- It is safer than motor oil [3].
- Its lubrication is more effective than motor oil [3].
- It is not flammable [3].
- It is an electrical insulator, which means it will increase the life of the RC car [3].
- It is usually cheaper than motor oil [3].

The term WT refers to the weight because what changes between one oil and another is the molecular mass. Changing the molecular mass means changing the viscosity, but it does not mean that a silicone oil WT35 has a density greater than one WT70. The density is always the same, only the chemical composition changes and therefore the viscosity. The amount of oil inserted into a front shock absorber in terms of volume and in terms of mass is always the same, but the volume changes between front and rear because the front ones are shorter than the rear ones.

## 2. Preliminary analysis

Tests were performed for 24 different oil-shock absorber configurations. For each configuration, 6 different possible ideal values of piston displacement amplitude were considered, and 4 tests were carried out for each of these, for a total of 24 tests per configuration. Once all the displacements were explored (6 iterations), the damper was changed with another one and the procedure was repeated from the initial point. To obtain a good repeatability and have the possibility to compare the results among them, the following acquisition data were chosen for all the tests in question:

- the initial frequency of 1 Hz.
- the final frequency of 20 Hz.
- the sweep rate of 0.2 Hz/s.
- the sample frequency of 1600 Hz.

So, considering the data obtained from the previous thesis the first task was to choose two representative configurations and extract in MATLAB the trends of the force impressed by the shaker to the damper and the piston travel versus the time, and then post processing them to find the damping force. The tests in question are tests number 4 of the 35WT and 70WT configurations as regards the front shock absorber, with 2 mm useful travel. Test 4 was chosen as it is certainly better than the previous tests and because it reflects reality more accurately. This is for two reasons: the first is that the oil has warmed up, therefore it has reached the actual conditions of use; the second is that, from one test to another, the driver, that is the control law of the test, is gradually more refined to obtain the desired displacement.

## 2.1 Force and displacement signals analysis

At the beginning the force and displacement signals of each test were saved as a vector together with the corresponding time, starting from the .mat files extracted from “TestLab”, that is the program in which the data of the tests are read. Then, since the signals are affected by a certain quantity of noise, they must be filtered, especially as the effect of noise increases with successive derivations, which will then be used for other calculations. The noise can be evaluated from the FFT diagram in Figure 2.1.1:

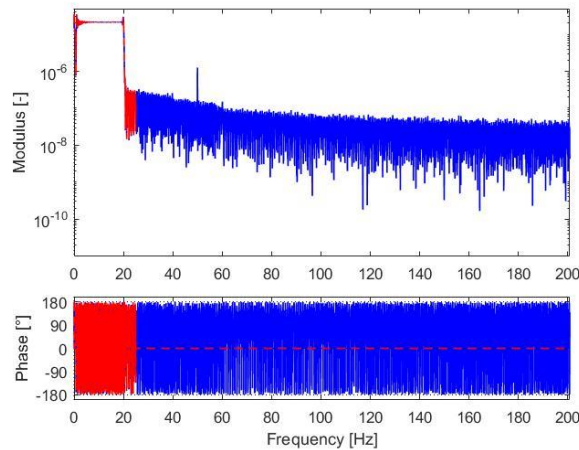


Figure 2.1.1 – FFT diagram of displacement signal 35WT.

Looking at the Figure 2.1.1 it is possible to see that everything after 20 Hz of frequency does nothing but dirty the signal, so the solution is to use a lowpass filter through a Matlab function called “Digifilt” to delete all the frequencies above a chosen threshold of 25 Hz. In addition, the time vector has been reduced to the interval of interest of the analysis, i.e., looking for the point where the frequency is close to 20 Hz in a stable way, which corresponds to the final time of interest of the test, through the moving mean of the average frequency, found as the inverse of each period of the signal. The start time was found by subtracting the total sweep period of 95 seconds from the final time obtained previously. From Figure 2.1.2 can be seen precisely the average frequency increasing in time with the corresponding moving mean of the values, with two black lines in correspondence of the instants of interest. There are also two magnifications in correspondence of the points of interest.

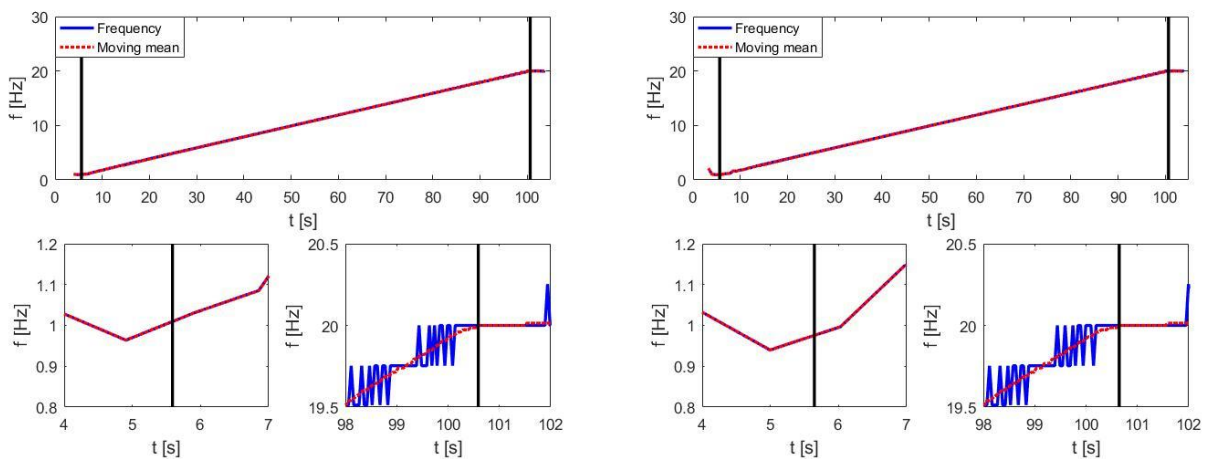


Figure 2.1.2– Test increasing frequency with the corresponding moving mean for 35WT (left) and 70WT (right).

Since for the moving mean a window of  $k = 18$  values have been taken into account, it has not been calculated for the first  $k$  values because there are no other values on the left side and the result would have been wrong. However, it can be seen how the initial trend is almost linear even without making the moving mean. It can be observed that the final time and the initial time for the sweep in the two tests are similar but not the same.

However, after finding the final time and the initial time, the values of the various signals were saved considering only the interval of interest for each test, and the time vector was offset to zero. From Figure 2.1.3, which shows an excerpt of the time history of the force and displacement of the 35WT test, we can understand that force and displacement have unanimous direction because a positive force peak is followed by a positive displacement of the piston. There is a delay in the response with respect to the input, which in this case is the force, as it should be. From the analysis of the previous thesis the direction of force and displacement in addition to being concordant is positive if upward.

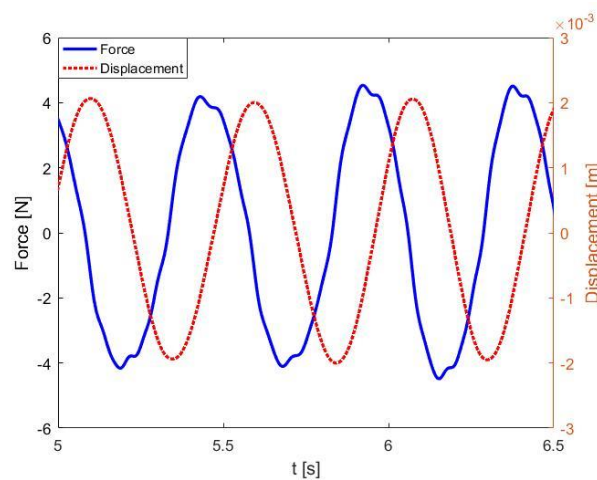


Figure 2.1.3 – Small time history of force and displacement 35WT.

From Figure 2.1.3 can be seen that the shape at the top of the signals is not regular even after filtering. This is due to the friction effect caused by the presence of the seals between the stem and the cylinder and by the contact between the piston and the cylinder walls, even if the elements are lubricated and immersed in oil. So, there is an effect of “stick-slip” as the piston reverses direction at the top and bottom of its' stroke, where the velocity is zero and there is the transition between static and dynamic friction. This effect creates irregularities of the signal in the initial peaks. It disappears at higher frequencies because the higher the velocities, the more the static friction time interval decreases.

Figure 2.1.4 shows the envelope of the forces exerted by the shaker over time, with the two lines that indicate the end and beginning of the sweep and enclose the time interval that will be considered.

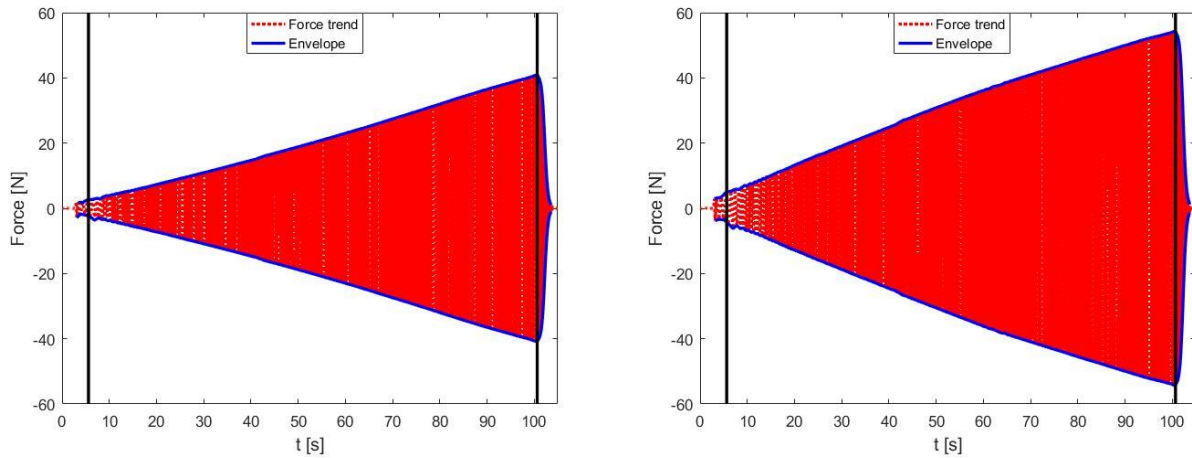


Figure 2.1.4 – Force trend in time domain and the corresponding envelope for 35WT (left) and 70WT (right), with imposed displacement of 2 mm.

In these two figures can be seen, just as expected, the clear difference in the force required on the system to obtain the same desired displacement if the oil viscosity is increased considerably.

To find the envelope of the curves it has been used a function called “findpeaks(data, x)”, which takes as inputs the displacement signal and the time and returns the values of the local maximums and their locations in time, indicating the minimum prominence of the peaks to be selected because there are irregularities in the first part of the signals, which if considered do not allow for a clean envelope. If the symmetrical signal with respect to the x-axis is given as input of this function, the function returns the values of the local minimums. At the end they are plotted together to form the envelopes.

For what concern the displacement, since there was a laser measurement offset, the average of the initial values of the test, where excitation is zero, was calculated and then this value was subtracted from the displacement at each point to make the test start from zero. Figure 2.1.5 show the envelope of the trends of the two piston displacements during the interval of interest of the tests.

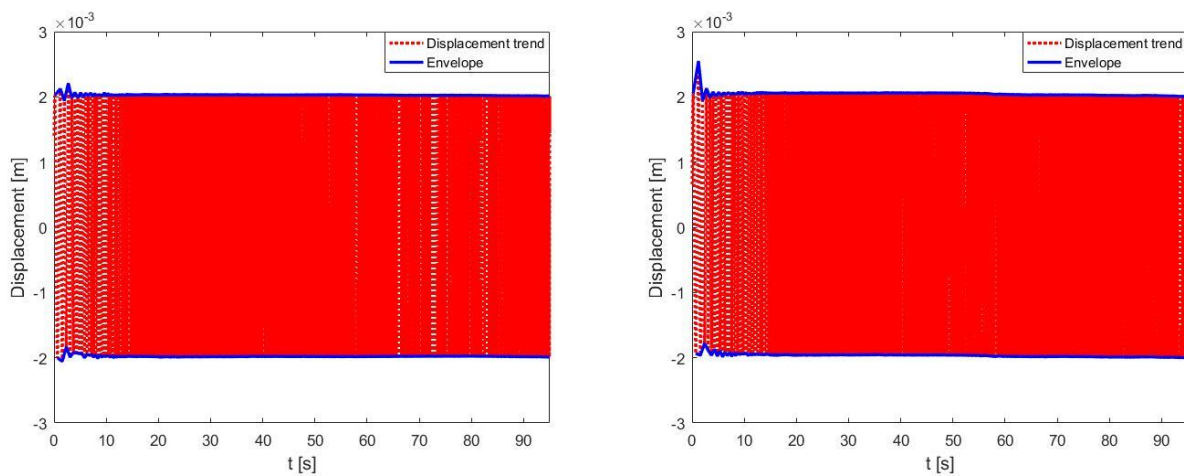


Figure 2.1.5 – Displacement trend in time domain with the corresponding envelope for 35WT (left) and 70WT (right).

Now in order to have the clearest possible graphs in the subsequent analyses, the upper and lower envelopes of the measured forces were compared in Figure 2.1.6.

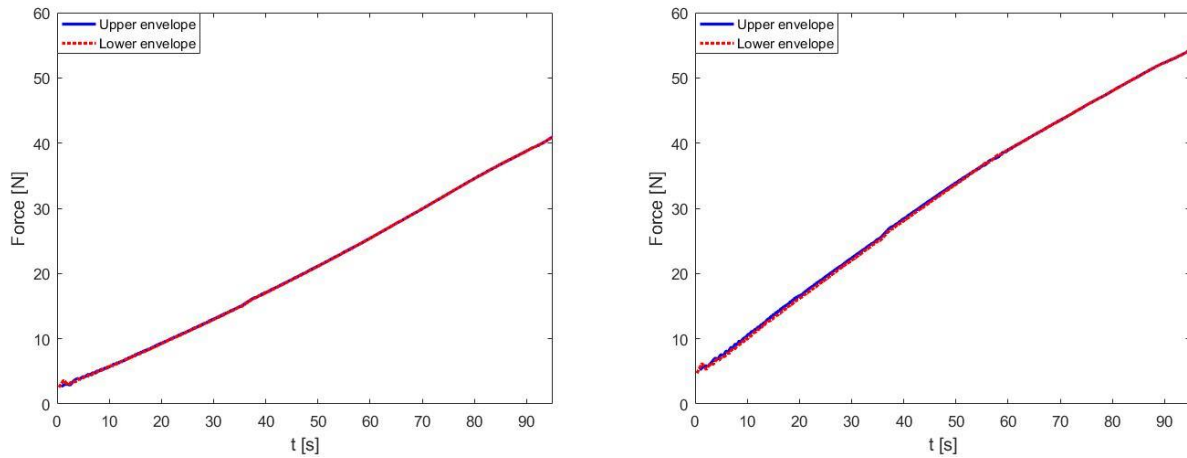


Figure 2.1.6 – Upper and lower envelope (considering the modulus) comparison of the force for 35WT (left) and 70WT (right), with imposed displacement of 2 mm.

As can be seen from the figures they correspond, so in the following it will be considered only the upper envelope for the analysis of the forces.

Subsequently, as shown in Figure 2.1.7, the time axis has been replaced with the corresponding frequency axis according to the acquisition data. The frequency vector, since the sweep starts from 1 and ends at 20 Hz, must be calculated with the equation 2.1:

- The values of frequency were calculated with the formula of the line passing through the points ( $f_1$ ;  $f_2$ ) for the frequency and ( $t_1$ ;  $t_2$ ) for the time, that is:

$$\frac{(f - f_1)}{(f_2 - f_1)} = \frac{(t - t_1)}{(t_2 - t_1)} \quad (2.1)$$

With:

- $f_1 = 1$  Hz.
- $f_2 = 20$  Hz.
- $t_1 = 0$  s (because the time vector has been offset to zero).
- $t_2 = 95$  s.

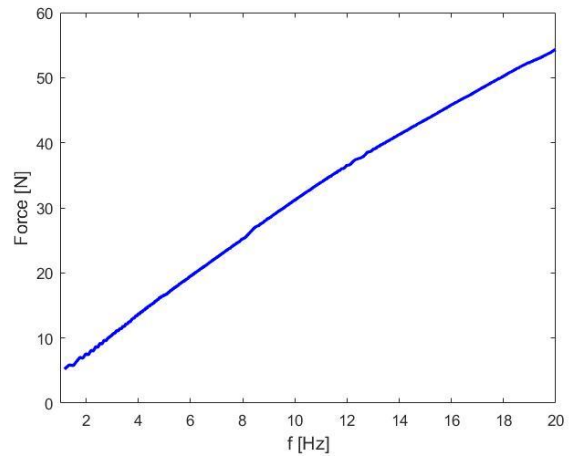
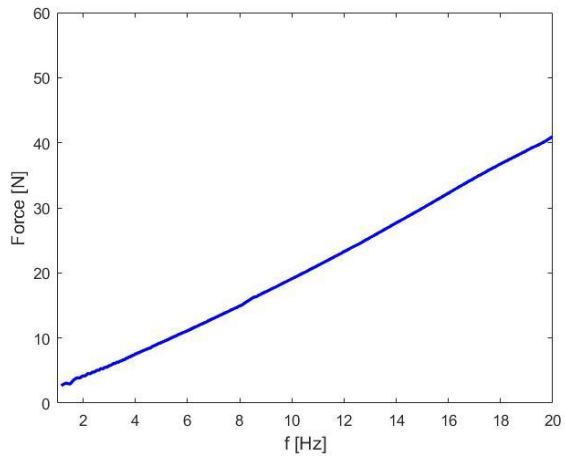


Figure 2.1.7 – Force envelope in frequency domain for 35WT (left) and 70WT (right), with imposed displacement of 2 mm.

## 2.2 Velocity and acceleration

In Figure 2.2.1 is reported the envelope of the displacement as function of the frequency for the two configurations taken into account, also considering the ideal case, that has been represented as the envelope of a linear chirp signal created using the MATLAB function “chirp(t, f1,T, f2)”:

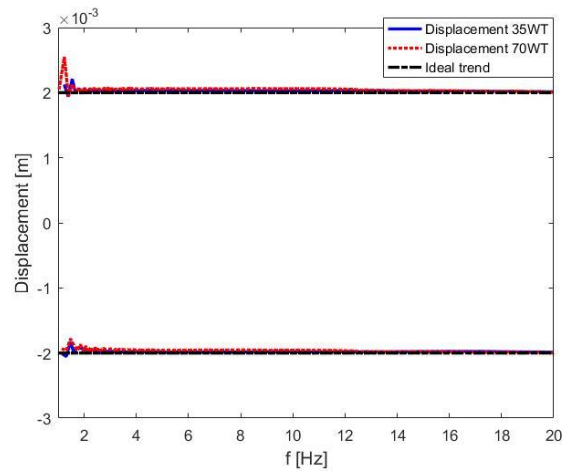


Figure 2.2.1 – Envelope of displacements in frequency domain for 35WT and 70WT.

The experimental velocities of the piston have been found deriving the experimental displacements and they are reported in Figure 2.2.2 as envelopes with the derivative of the chirp signal found before.

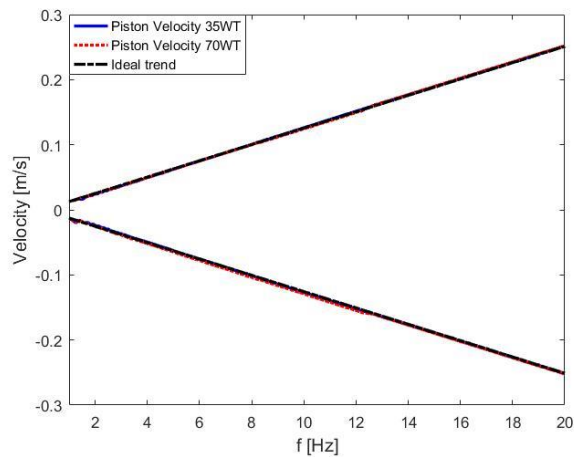


Figure 2.2.2 – Envelope of velocities in frequency domain for 35WT and 70WT.

For what concern the acceleration, that is needed to find the inertia force, it has been found as a derivative of the velocity and it is represented in Figure 2.2.3 for the two configurations.

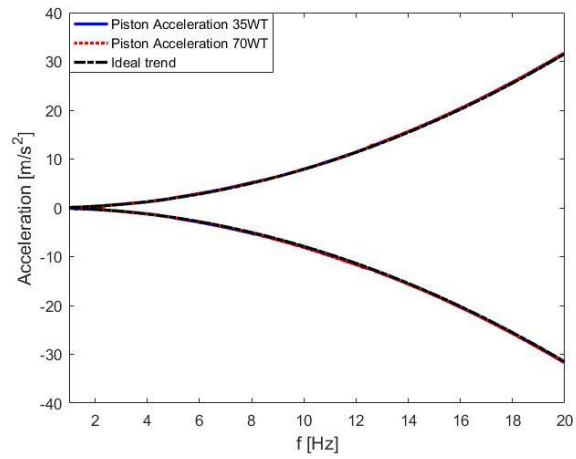


Figure 2.2.3 – Envelope of accelerations in frequency domain for 35WT and 70WT.

From these graphs it can be seen that the envelope of the numerically created signal and that of the experimental signals derived point by point coincide perfectly.

## 2.3 Experimental damping force

Through the free body diagram in Figure 2.3.1 (right), it can be seen how the force that the shaker apply to the system is equal to the sum of the damping force of the shock absorber, which is expected to be the prevailing contribution, plus an inertial contribution due to the moving masses.

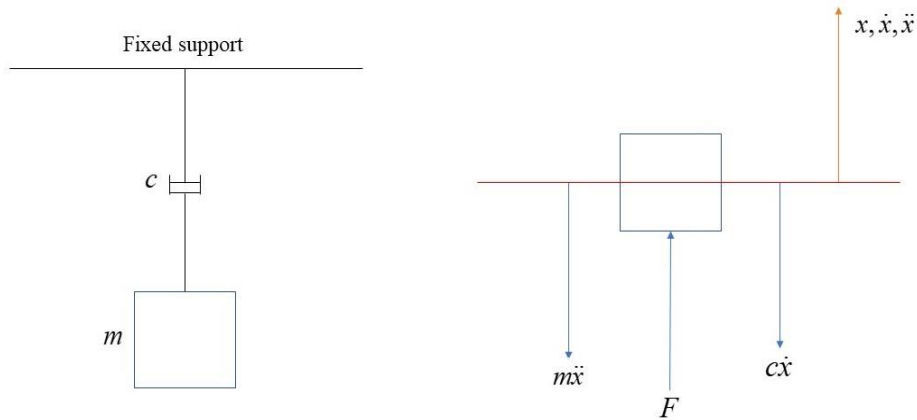


Figure 2.3.1 – Physical scheme (left) and free body diagram (right).

To find the damping force, first it is important to understand which are the moving components between all system elements that are represented in Figure 2.3.2 and obtain the sum of the masses.

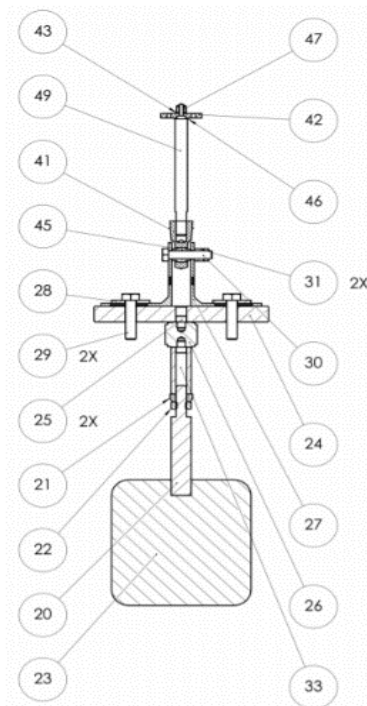


Figure 2.3.2 – Section view of the system [1].

In the analysis the liquid inside the shock absorber will not be considered as a moving element. As the force reading information corresponds to the point at which the load cell is located, only the elements above it should be considered as inertial contributions.

These elements have been cataloged in the following Table 2.3.1, where each component is identified by a number with which it is associated in Figure 2.3.2:

Table 2.3.1 – List of moving elements.

Part number	Description	Rear	Front
		Mass [g]	Mass[g]
24	Main stirrup	249.46	249.46
25	2x M6/10-32 adapter	2.76	2.76
27	2x 'L' stirrup	29	29
28	2x M5 washer	6.4	6.4
29	2x M5 screw	7.6	7.6
30	M5 screw	3.8	3.8
31	2x M5 nut	2	2
41	Spheric joint	2.4	2.4
42	Piston	2.2	2.2
45	M5 screw cross key	5.3	5.3
43-46-47-49	Stem (with washers and M2 bolt)	30	22.3
Not in drawing	Rubber cap	2.7	2.3
<b>TOTAL</b>		<b>343.62 g</b>	<b>335.52 g</b>
		<b>0.3436 kg</b>	<b>0.3355 kg</b>

As it is possible to notice the largest contribution comes from the main stirrup, but all the other components have a weight that is important to not neglect.

Once the moving mass and the acceleration are known, multiplying them point by point, the trends of the inertia forces can be found. Finally, it is possible to resolve the dynamic balance subtracting the inertia force from the measured force punctually through the formula 2.3.1:

$$c\dot{x} = F - m\ddot{x} \quad (2.3.1)$$

and obtain the damping force trend in the two cases as shown in Figure 2.3.3, where all the forces are represented as an envelope.

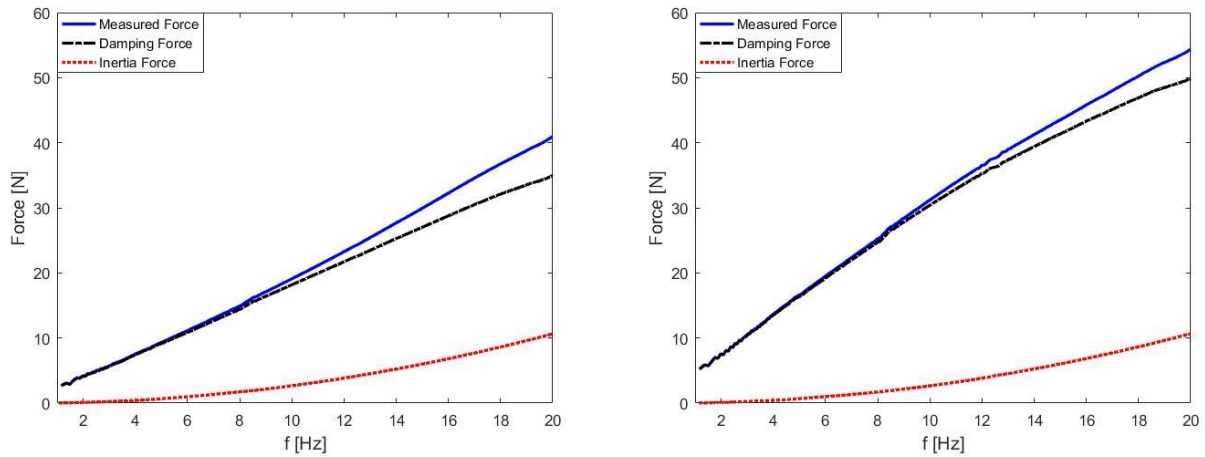


Figure 2.3.3 – Upper envelope of the measured, damping and inertia force in frequency domain for 35WT (left) and 70WT (right), with imposed displacement of 2 mm.

Of all the force measured due to the system we have a rather negligible inertia around the first 6-8 Hz and then its effect becomes increasingly important. For greater clarity, in Figure 2.3.4, time histories of the forces are also given.

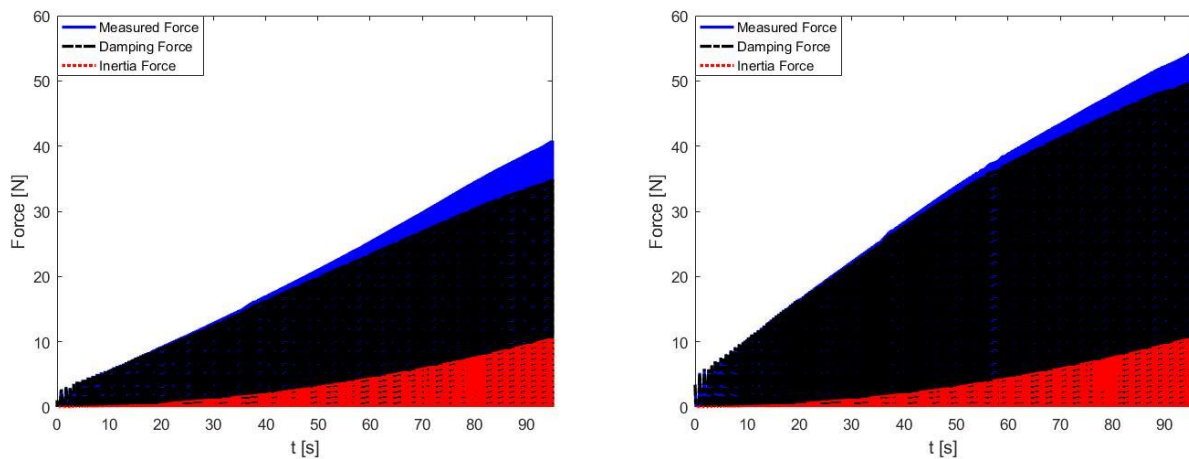


Figure 2.3.4 – Positive trend of the measured, damping and inertia force in time domain for 35WT (left) and 70WT (right), with imposed displacement of 2 mm.

From these graphs removing the contribution of the mass results in a non-linear damping force as it deviates from a straight line. While the velocity is quite linear as an envelope, the force  $c\dot{x}$  should be linear and is not. Another difference is that the measured force trend itself becomes non-linear at higher velocities for 70WT configuration because of the viscosity of the oil that is doubled.

Now, before obtaining the damping coefficient by dividing the damping force by the velocity point by point through the formula 2.3.2, it is necessary to consider only velocities exceeding an absolute minimum value, which is set at  $v = 0.01$ , which is approximately the initial absolute value of the velocity envelope.

The results are represented in Figure 2.3.5, which also shows a magnification of points in a small frequency range between 15 and 15.03 Hz.

$$c = \frac{F_{damp}}{\dot{x}} \quad (2.3.2)$$

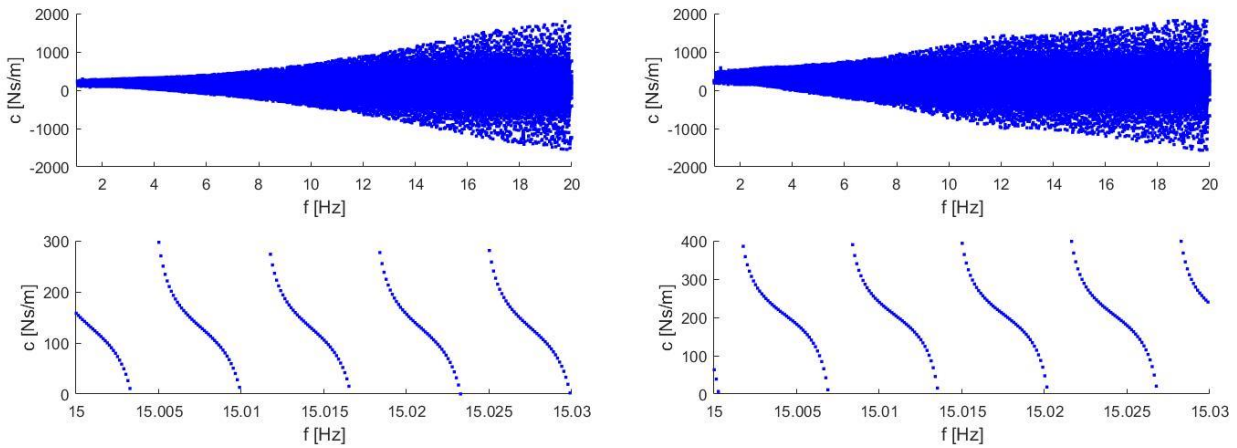


Figure 2.3.5 – Damping coefficient trend for 35WT (left) and 70WT (right), with imposed displacement of 2 mm.

From these graphs we see that by enlarging the y-axis the points corresponding to the damping coefficient oscillate with periodic discontinuity around an average value ranging from 0 to 200 Ns/m for the 35WT and from 100 to 300 Ns/m approximately for the 70WT. The fact that increasing oil viscosity for the same imposed displacement also increases the mean damping coefficient has been verified.

## 2.4 Interpolation of the damping force

Now it's possible to evaluate the theoretical damping force with a Matlab function called "PolyLMS", that is an interpolating function, that takes as inputs the velocity, the damping force and the active coefficients that are needed and gives the damping coefficients of the function.

Before interpolating, since is needed a wide frequency range and there are so many signal points, interpolation would be too slow, so is necessary to down sample the force and velocity signals. In this case the sampling frequency has been halved in 800 Hz. Figure 2.4.1 shows the points of the original force signal with the resampled signal in a certain interval to show that they coincide.

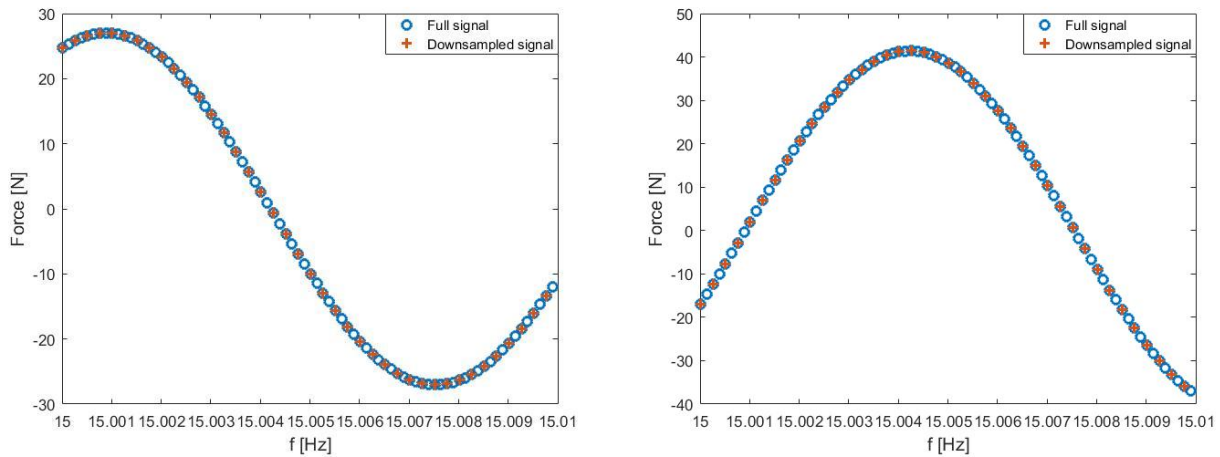


Figure 2.4.1 – Original and down sampled signal points in a small interval of frequency for 35WT (left) and 70WT (right), with imposed displacement of 2 mm.

The results for the two tests, having chosen as interpolation interval the values in the frequency range from 5 to 15 Hz, are reported in Figure 2.4.2, which show the damping force interpolated with three different coefficients configurations together with the computed damping force. The coefficients found through interpolation were multiplied by the numerical velocity found by deriving the previously created chirp signal.

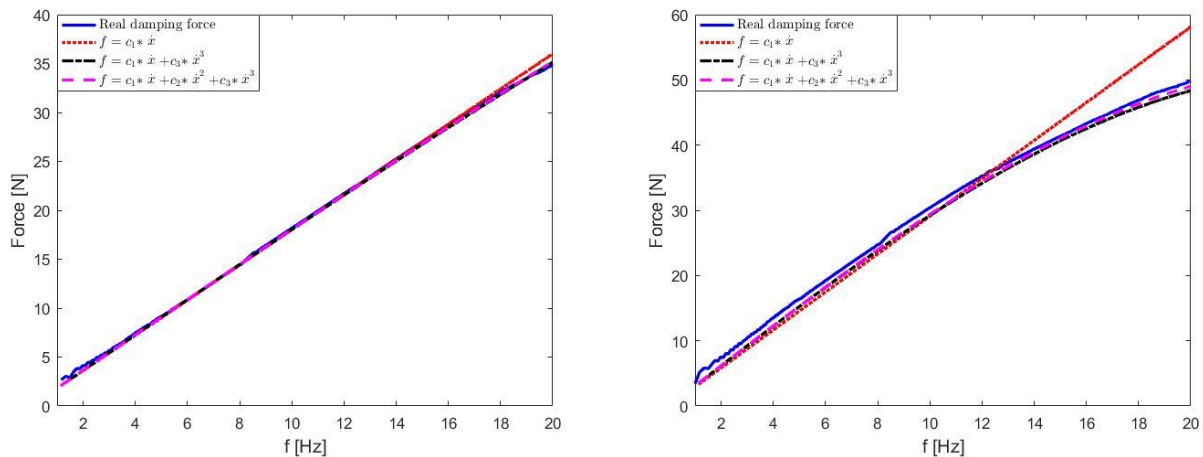


Figure 2.4.2 – Computed damping force interpolation with three different sets of coefficients for 35WT (left) and 70WT (right), with imposed displacement of 2 mm.

From these figures we can make a qualitative comparison of the curves, but to make a quantitative comparison it is necessary to compare the coefficients and analyse another parameter, again obtained using the "PolyLMS" function, i.e. the mean square error given by the difference between the real and the interpolated curve.

### 2.4.1 Damping coefficients and interpolation error

To determine which set of coefficients is the best, one must look at the weights that the different coefficients have, so Figure 2.4.1.1 shows the values of the three coefficients in the case of the complete cubic polynomial for 35WT and 70WT.

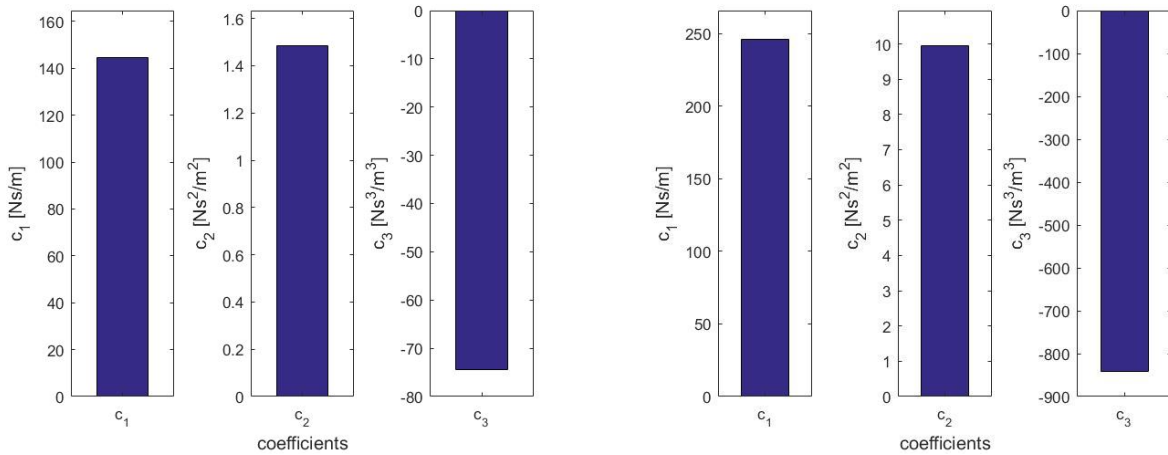


Figure 2.4.1.1 – Damping coefficients of the complete cubic polynomial  $c_1$ ,  $c_2$  and  $c_3$  for 35WT (left) and 70WT (right), with imposed displacement of 2 mm.

From these graphs, the weight of  $c_2$  is very small compared to the other coefficients, so it can be eliminated and the polynomial with the even term can be disregarded.

You can now move on to analyse the quantitative error of the interpolation in Figure 2.4.1.2 errors for 35WT and 70WT.

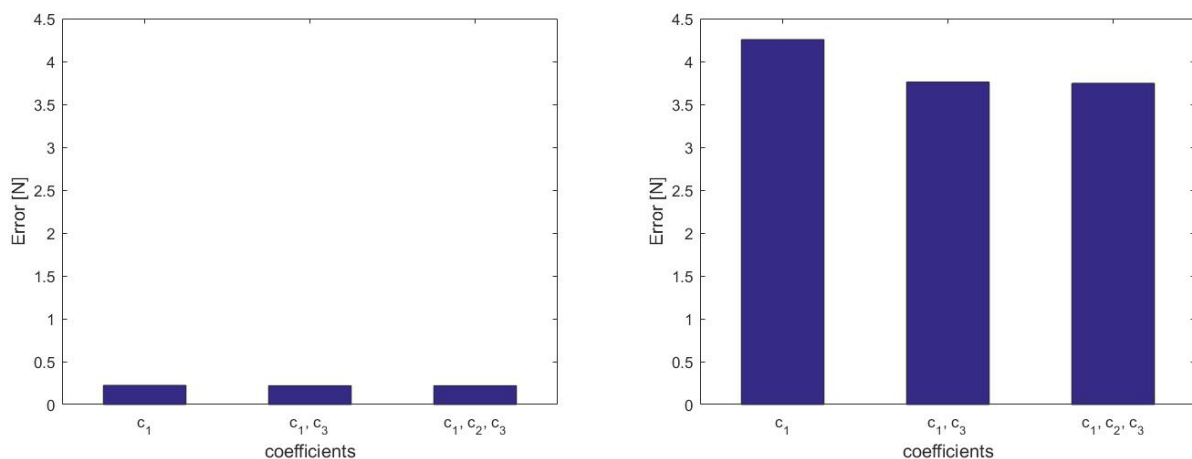


Figure 2.4.1.2 – Mean square error of the interpolation for 35WT (left) and 70WT (right), with imposed displacement of 2 mm.

Considering that the difference in error between the complete cubic and the cubic without  $c_2$  is almost non-existent, it is always better to consider the second one as the best interpolation like it was said before but considering the polynomial with the linear term and the cubic polynomial with odd coefficients, the error is lower in the second case especially for the 70WT case where the force has a less linear trend, so it will be taken as the best interpolating set.

For the interpolation graphs the envelope has been analysed, but for a complete analysis in Figure 2.4.1.3 the trends of the real damping force with the respective interpolated data in time domain are shown, taking into consideration only the best set of coefficients.

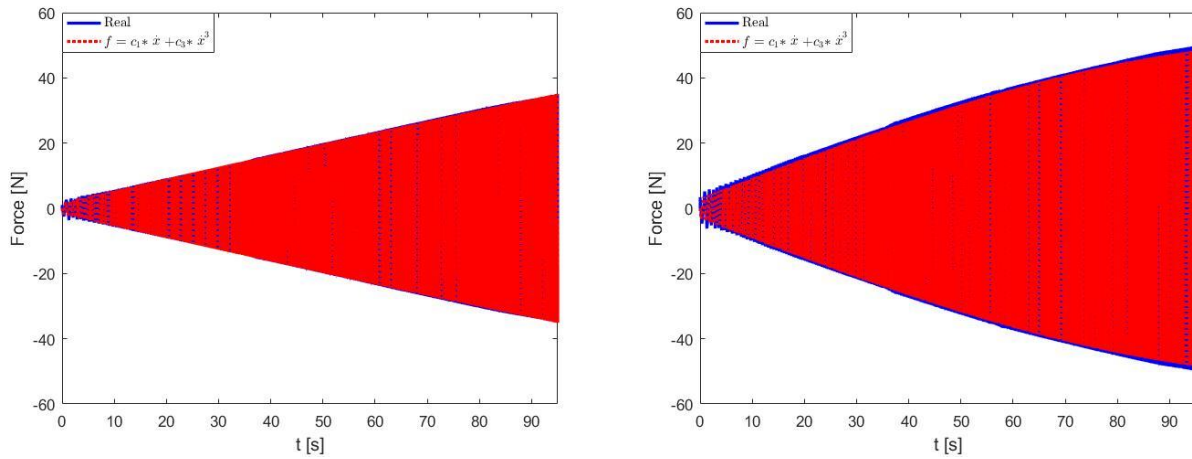


Figure 2.4.1.3 – Comparison between computed and interpolated damping force trend with the best set of coefficients for 35WT (left) and 70WT (right), with imposed displacement of 2 mm.

### 3. Frequency effect on damping coefficients

To see if there is an effect of frequency on the damping coefficients found through interpolation, other frequency ranges must be chosen within which to interpolate the damping force. In this case were considered the 35WT and 70WT configurations with 2 mm of displacement because if the stroke is too small, and the signals are not very clean. As shown in Figure 3.1, the three intervals of frequency are 3-8 Hz, 8-13 Hz and 13-18 Hz.

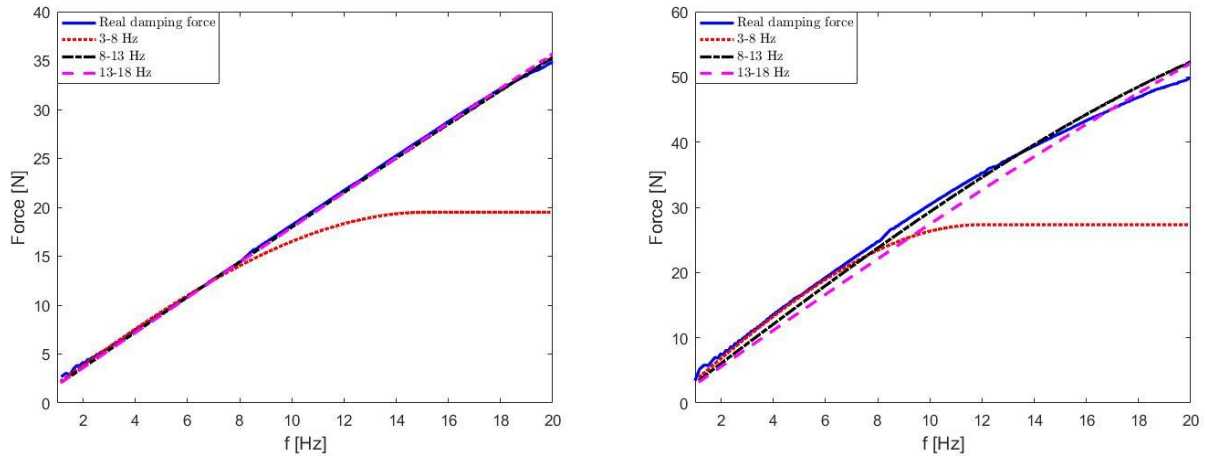


Figure 3.1 – Computed damping force interpolation considering three different intervals of frequency for 35WT (left) and 70WT (right), with imposed displacement of 2 mm.

From the Figure 3.2, which shows the damping coefficients of the interpolation, there is a dependency between the coefficients and the frequency range chosen.

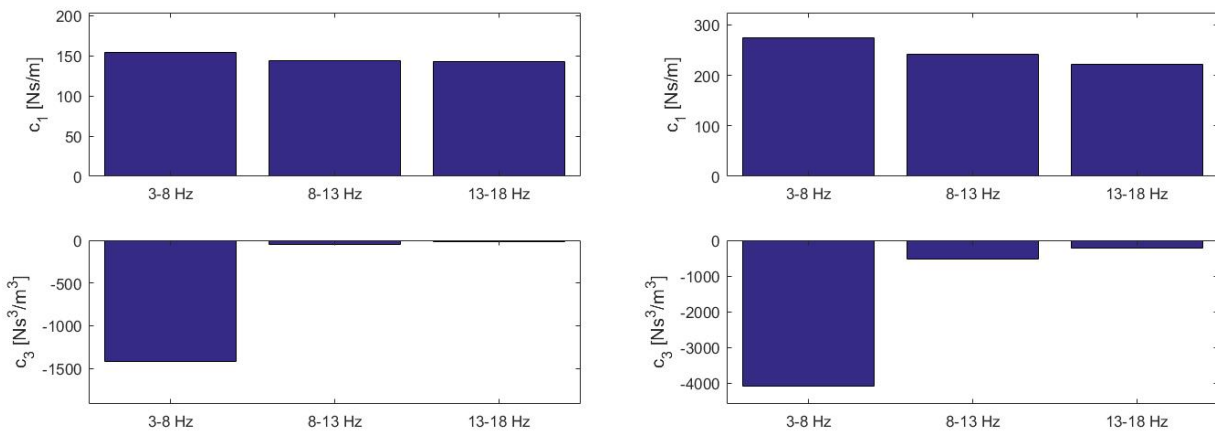
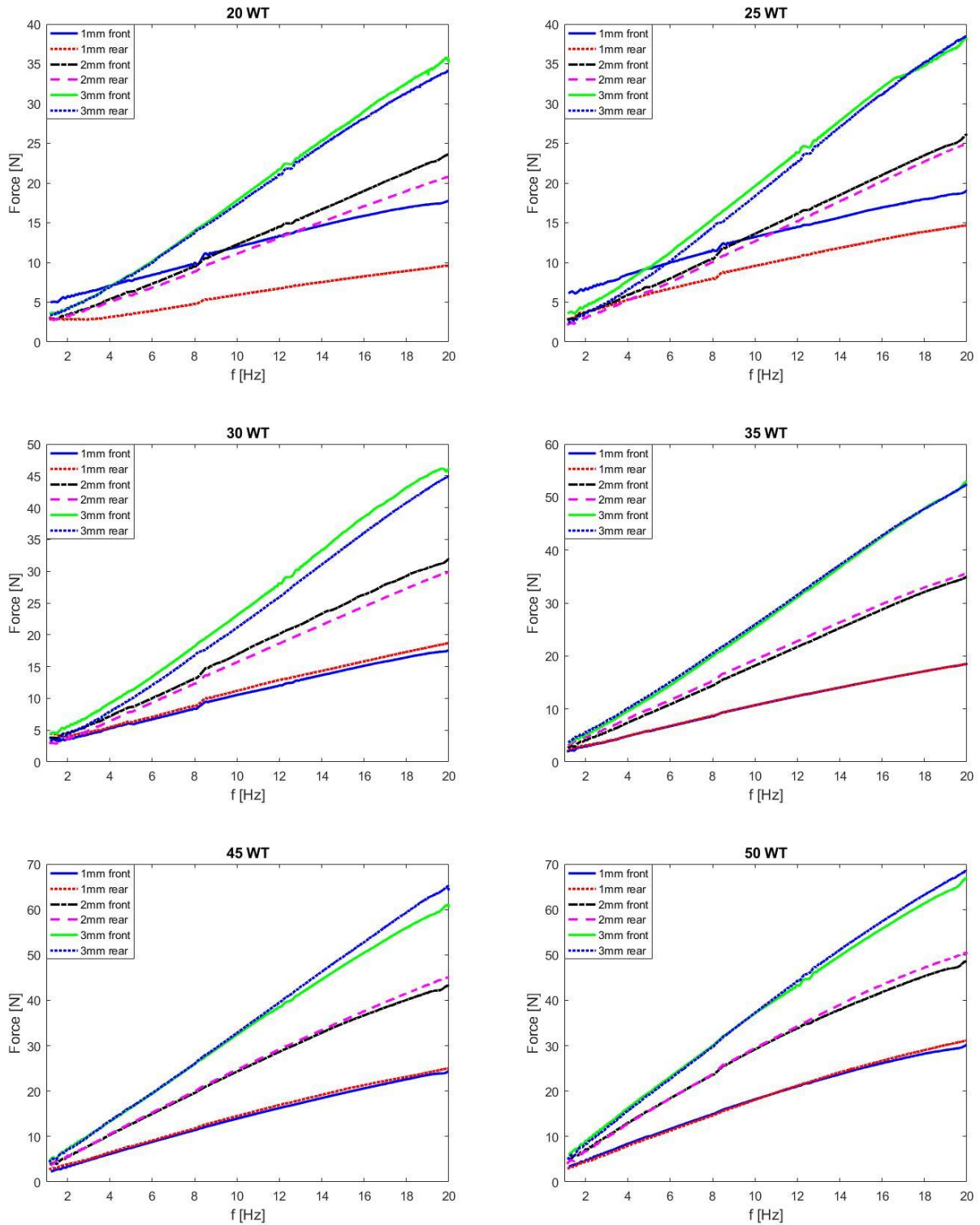


Figure 3.2 – Damping coefficients of the polynomial  $c_1$  and  $c_3$  considering three different intervals of frequency for the interpolation for 35WT (left) and 70WT (right).

The dependence of  $c_1$  on frequency is very low as it decreases with the increase of frequency of very little, whereas for  $c_3$  the gap between the first and second interval is very marked, but the second and the third are very similar in value.

## 4. Comparison between front and rear

Now, to see if something went wrong in some tests and if the two shock absorbers react in the same way, a comparison was made between the experimental damping force of the front shock absorber with the rear one, for three different displacements of 1 mm, 2 mm, and 3 mm. In order to have a complete analysis all the oil gradations have been considered. The results are reported in Figure 4.1.



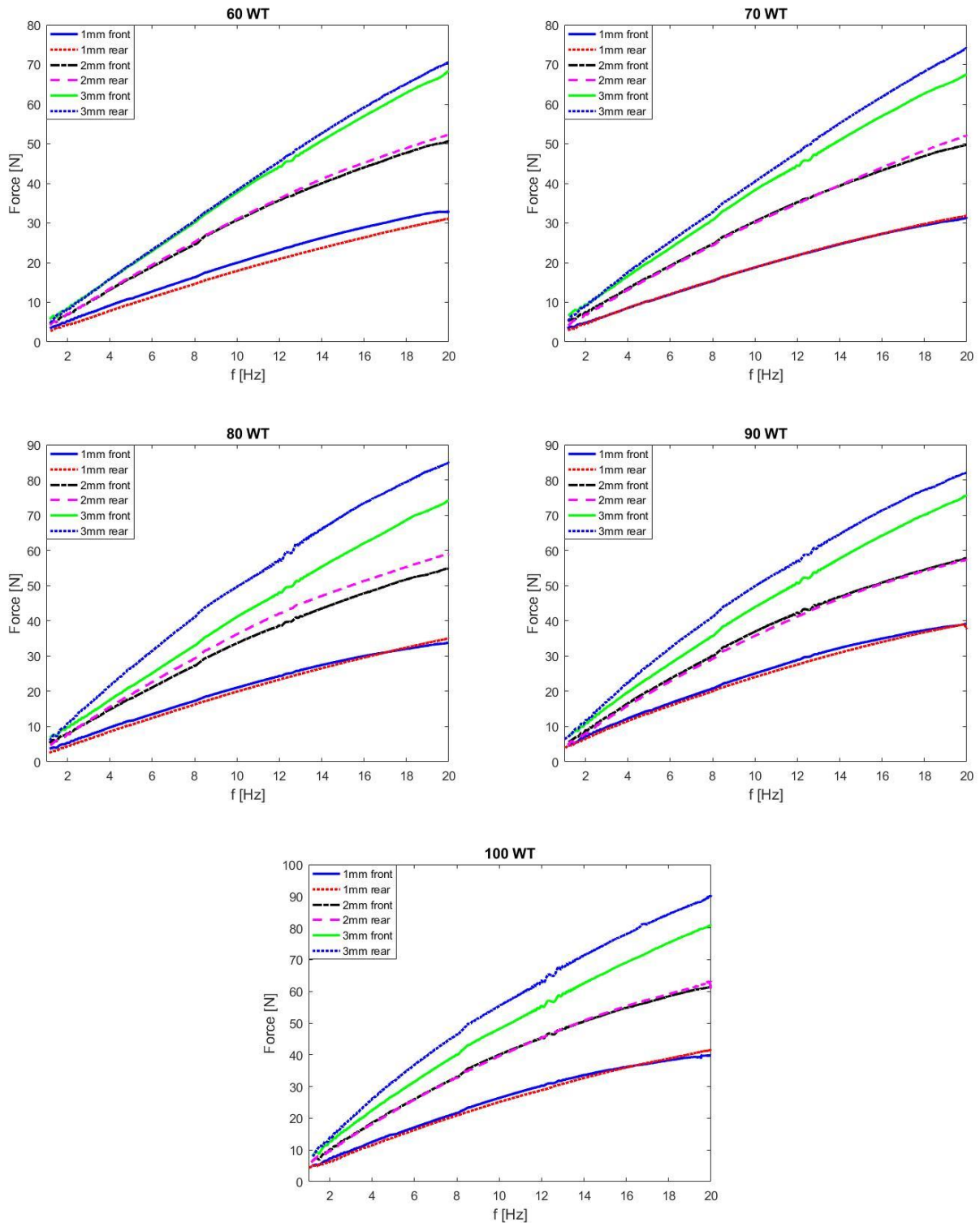
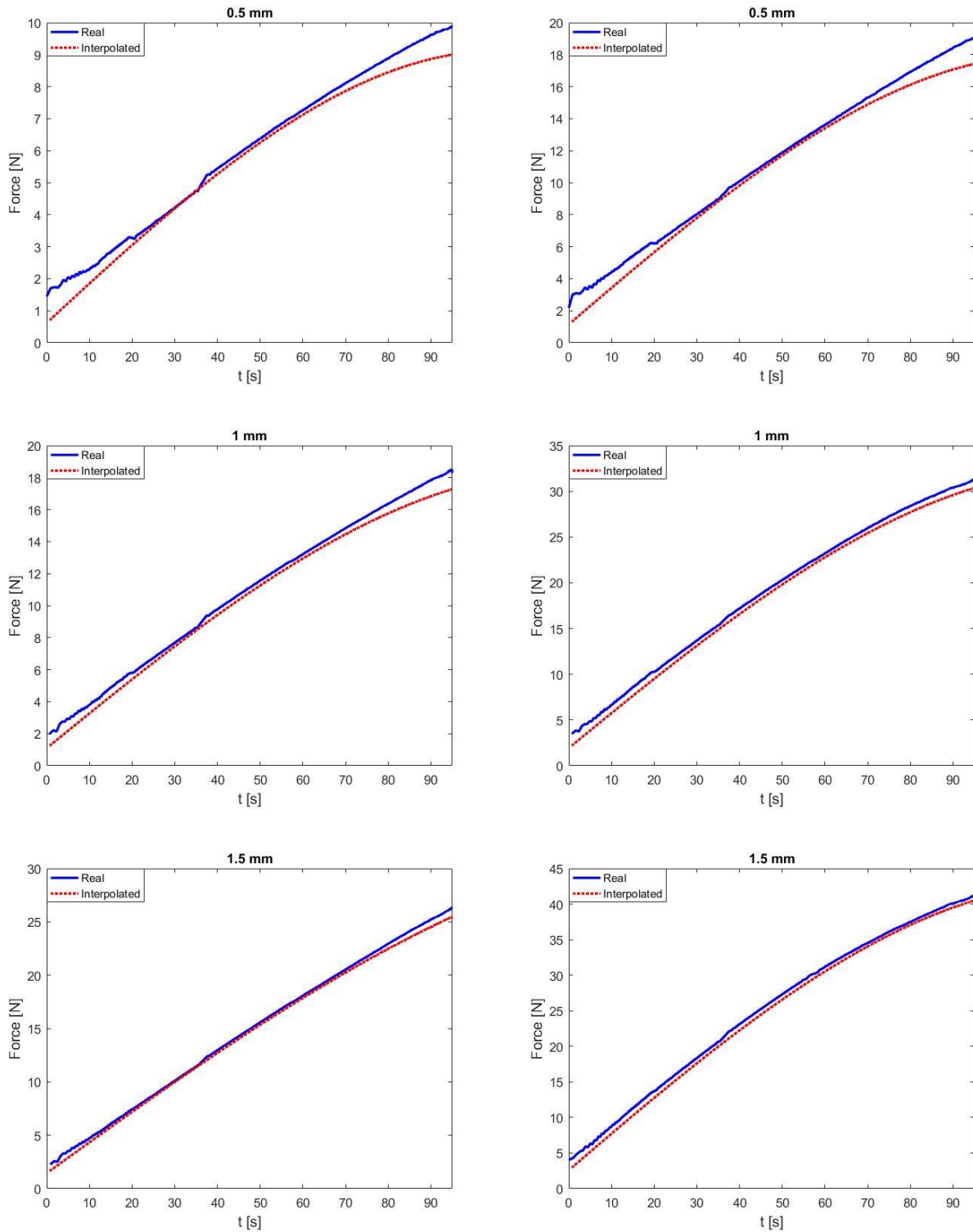


Figure 4.1– Damping forces upper envelopes considering the displacements 1mm, 2mm, 3mm for all the viscosities.

From these graphs for low viscosities and low displacements the damping force of the front shock absorber is clearly higher than the rear shock absorber, as in the case of 20 WT and 25 WT with 1 mm of imposed displacement. As the viscosity is gradually increased, the front and rear dampers always react in the same way, except in the cases of 70 WT, 80 WT, 90 WT and 100 WT with 3 mm displacement, where the damping force of the rear damper is always higher than that of the front damper by about 5-10 N.

## 5. Comparison between different piston displacements

Now taking into account the best set of coefficients, i.e., the case of the cubic polynomial with only odd terms, three different displacements for the two oil grades of 35WT and 70WT were analysed in Figure 5.1, to see the difference between the envelope of the real and the interpolated damping force.



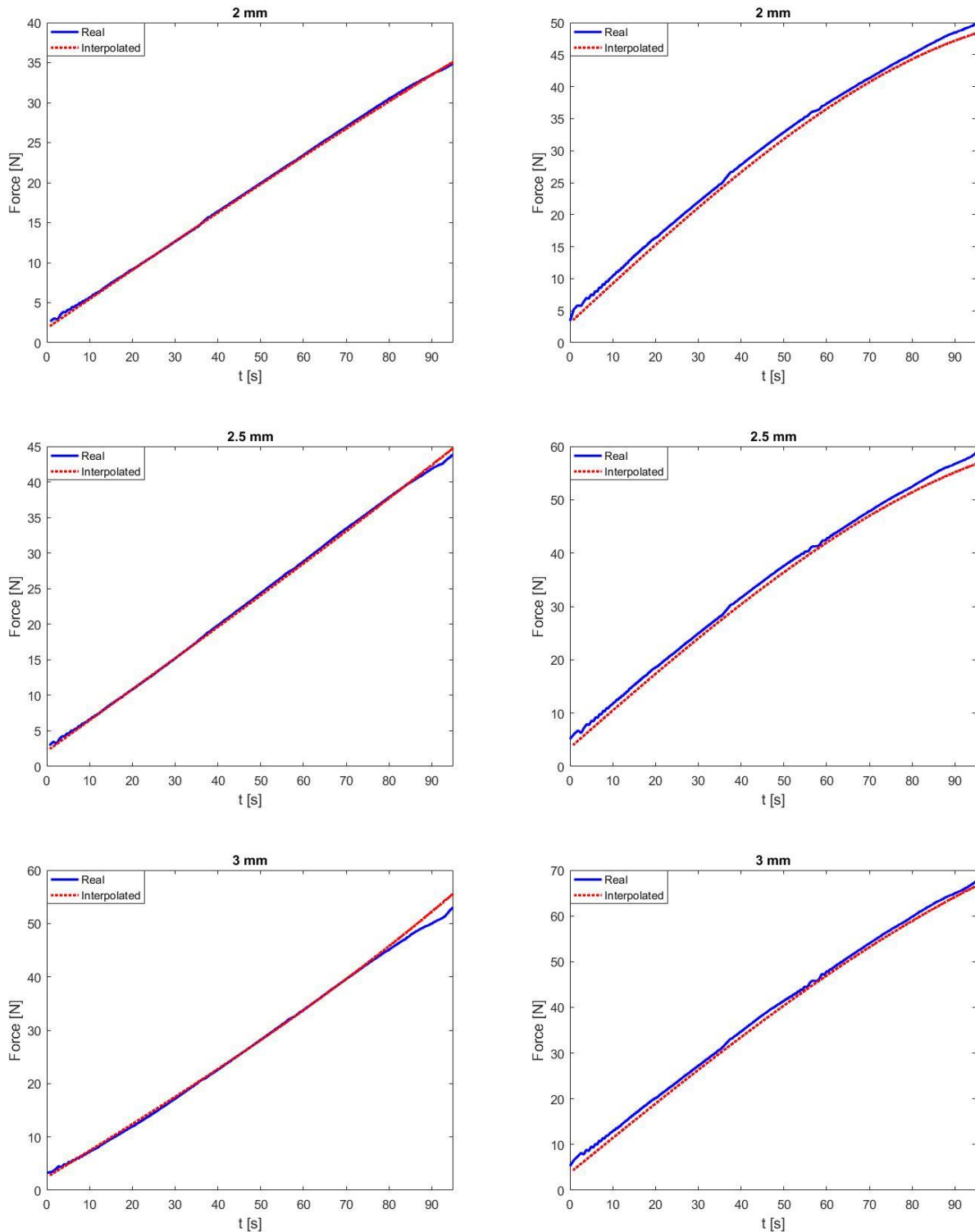


Figure 5.1 – Real and interpolated damping forces in time domain considering the displacement 1 mm, 2 mm, and 3 mm for 35WT (left) and 70WT (right).

For these graphs, it can be seen that the curves are separated by some small offset in some sections, while in others they are almost coincident or differ from the actual curve by only a few newtons, especially in the case of 0.5 mm of displacement, because the real curve is more irregular. However, the interpolation approximates the damping force very well and therefore it can also be said that the damping coefficients derived from interpolation can be analysed for different displacements and viscosities to find a dependency.

## 5.1 Damping coefficients for different displacements

Before considering the best interpolating set, the change of  $c_1$  and  $c_3$  if the set of coefficients for the polynomial is changed must be checked, as shown in Figure 5.1.1 for 35WT and in Figure 5.1.2 for 70WT.

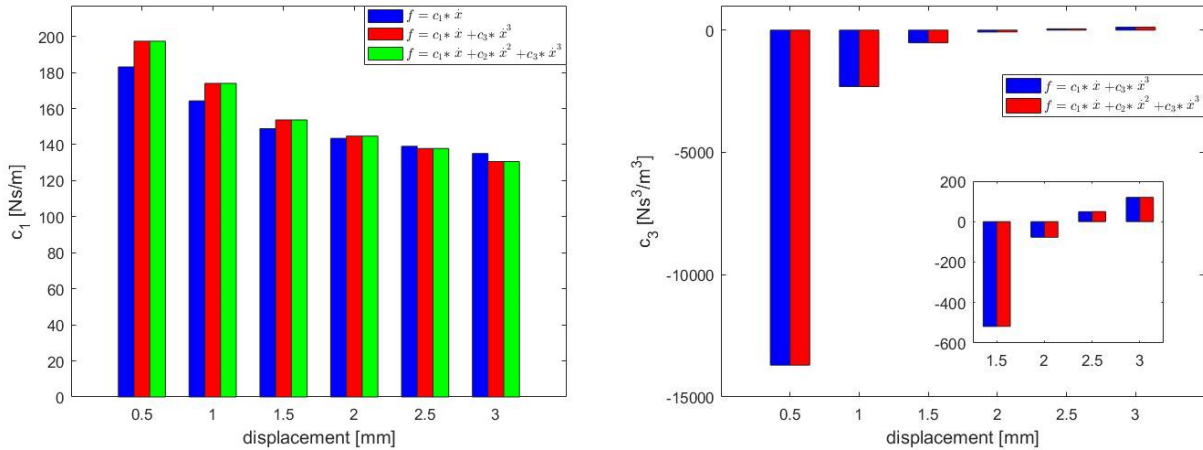


Figure 5.1.1 – Damping coefficients  $c_1$  (left) and  $c_3$  (right) for the three polynomials considering all the displacements for 35WT.

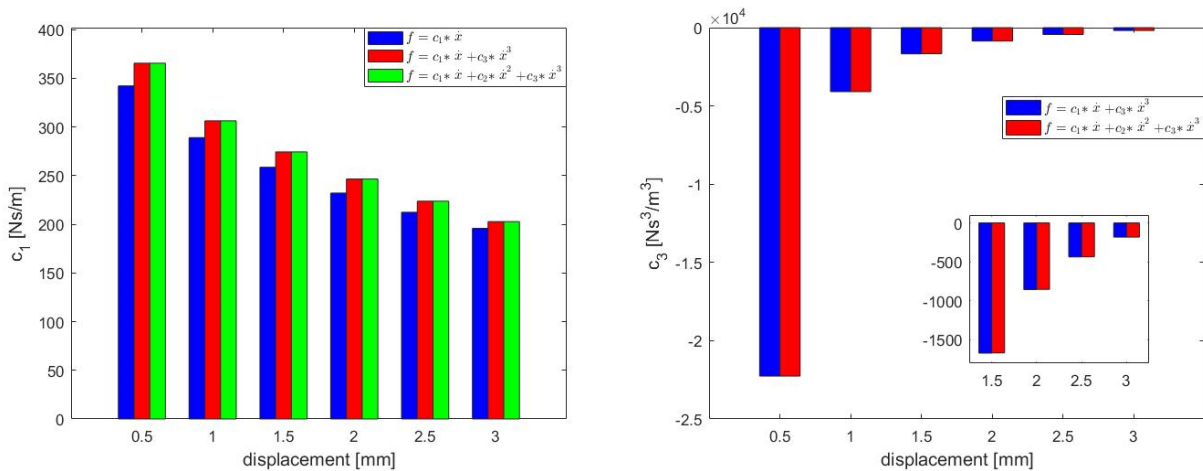


Figure 5.1.2 – Damping coefficients  $c_1$  (left) and  $c_3$  (right) for the three polynomials considering all the displacements for 70WT.

It can be seen how the coefficient  $c_3$  remains unchanged while  $c_1$  for cubic polynomials remains unchanged but is slightly lower for the polynomial with the linear term only.

Now, considering the best interpolating set for the damping force found before, to have a comparison between the two viscosities and to better see if there is a dependence with the displacement, the coefficients of the polynomial at different displacements have been reported in a bar chart in Figure 5.1.3 and Figure 5.1.4 respectively for the 35WT and 70WT oil, always taking into account the front shock absorber.

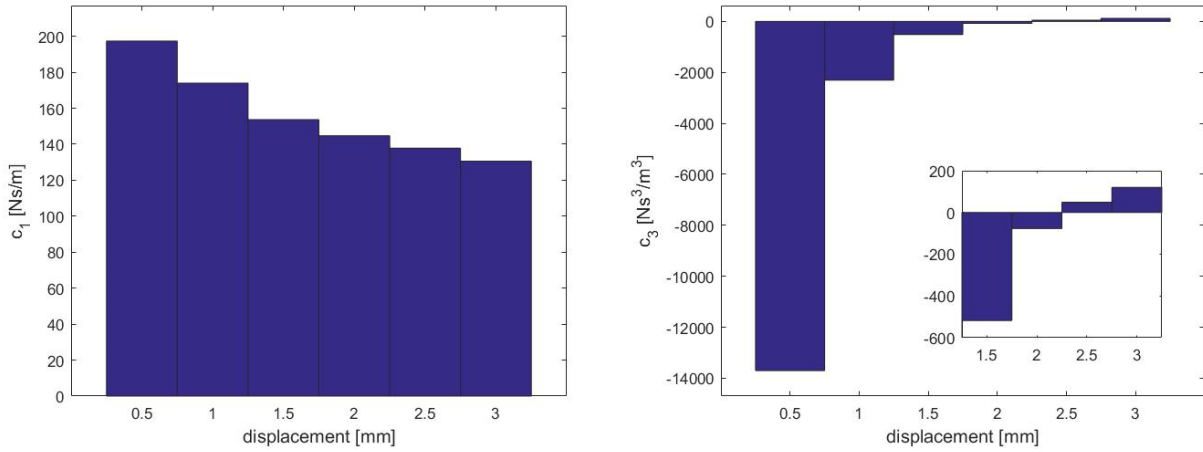


Figure 5.1.3 – Damping coefficients of the polynomial  $c_1$  (left) and  $c_3$  (right) considering all the displacements for 35WT.

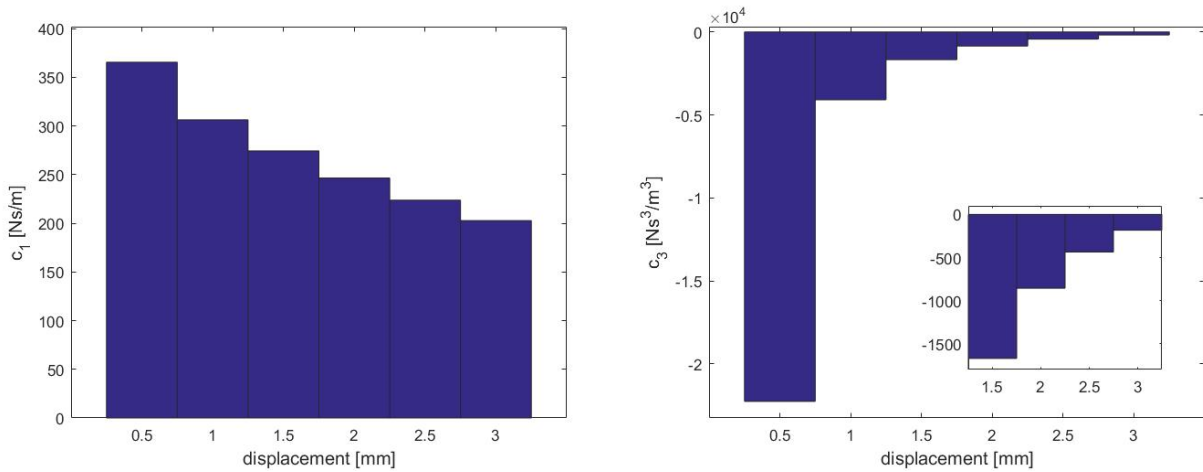


Figure 5.1.4 – Damping coefficients of the polynomial  $c_1$  (left) and  $c_3$  (right) considering all the displacements for 70WT.

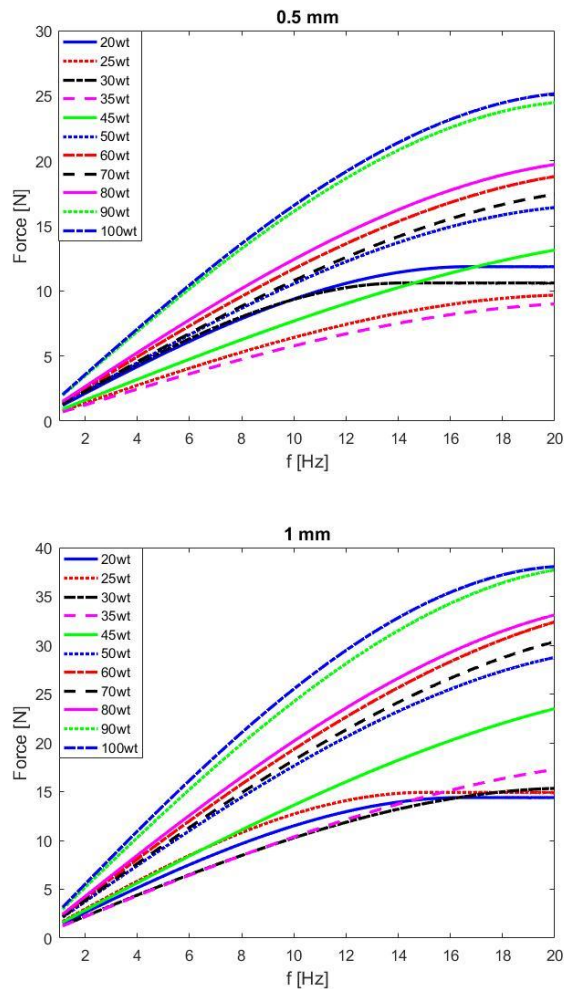
From these graphs it is evident that the damping coefficient  $c_1$  decreases with increasing displacement in a quite linear way from a certain value greater than zero, while the coefficient  $c_3$  is always negative under all amplitude conditions, except for the 2.5 mm and 3 mm case of the 35WT where it goes slightly above zero, and the absolute value decreases increasing the displacement. Moreover, it has an important weight especially for low amplitudes.

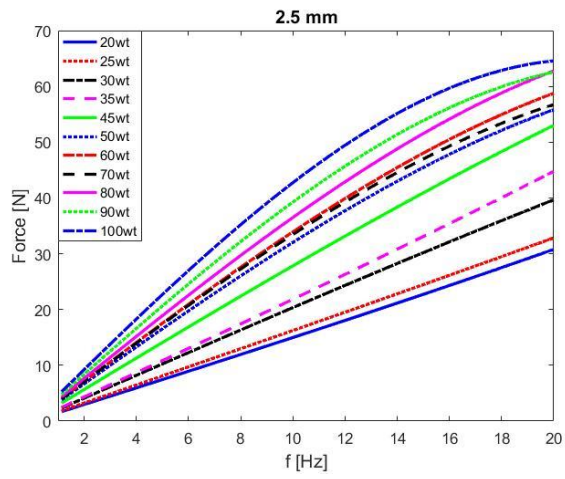
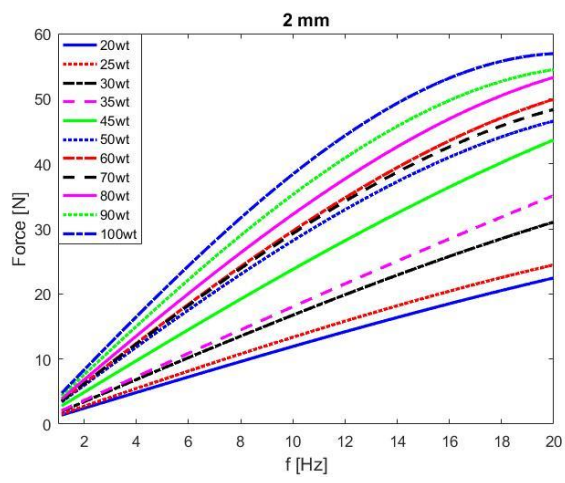
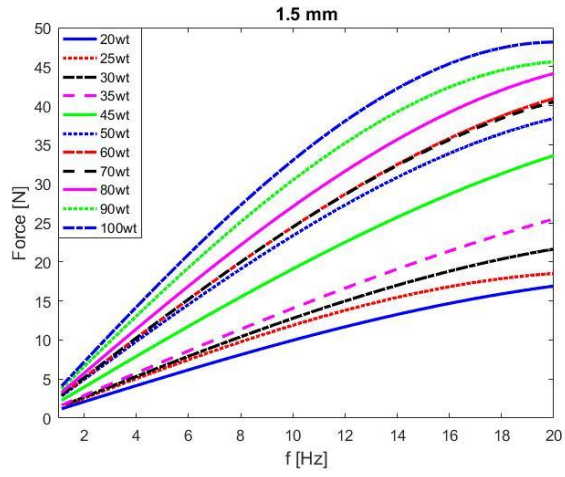
## 6. Comparison between different oil viscosities

So far, only two grades of oil for the front damper case have been considered in the study, so now the other configurations will also be taken into account.

Therefore, considering the test number 4 as regards the front shock absorber, with 0.5 mm of useful travel, for 11 different oil configurations, interpolated damping forces can be compared. In Figure 6.1 are represented the upper envelopes of all the damping forces.

In the cases of low displacements, even taking into account the last test performed, some viscosities gave wrong results because the piston stroke was too short, and in fact this will also result in errors with regard to the damping coefficients.





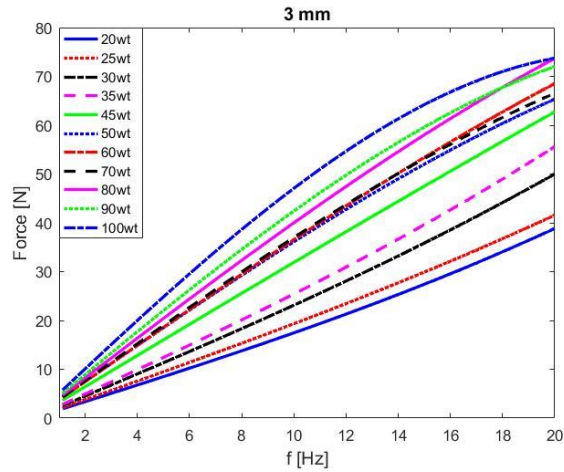


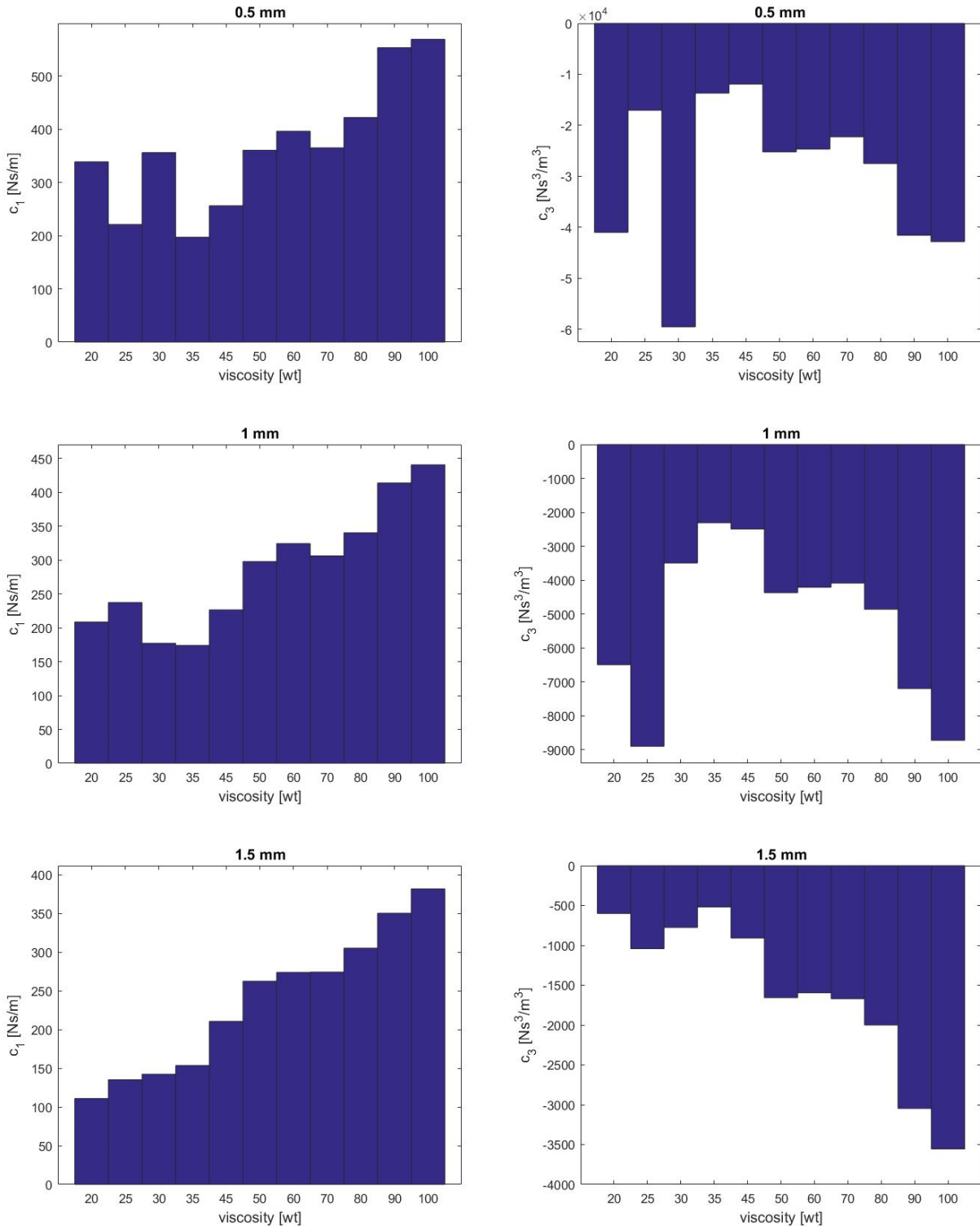
Figure 6.1 – Interpolated damping forces considering all the displacements for all the viscosities regarding the front shock absorber configuration.

In the cases of 0.5 and 1 mm displacement, lowest viscosities of 20WT, 25WT and 30WT gave problems as the stroke was too small. By further increasing the imposed piston displacement, it can be seen that the curves become more and more evenly distributed.

One problem concerns 70WT oil for all the displacements, because its envelope is always lower or almost coincident with 60WT. After checking that test number 4 was indeed the best test, this can probably be a problem with either shock absorber.

## 6.1 Damping coefficients for different viscosities

In addition to comparing forces, a comparison must also be made between the damping coefficients for different oils with the same imposed displacement, that are shown in Figure 6.1.1 for 0.5 mm, 1 mm, 1.5 mm, 2 mm, 2.5 mm, and 3 mm of imposed displacement for the front shock absorber since it always reacts in the same way.



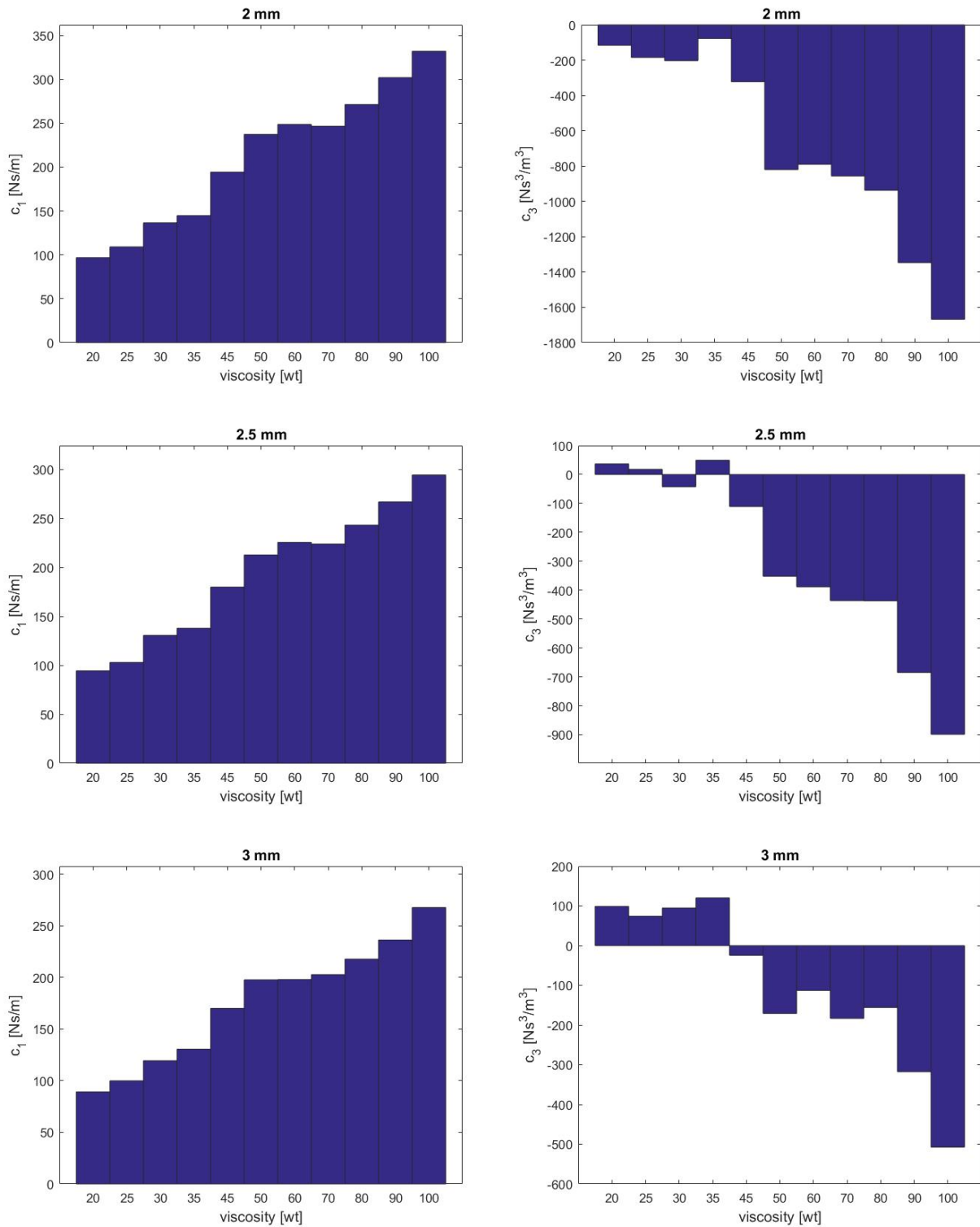


Figure 6.1.1 – Damping coefficients of the polynomial  $c_1$  (left) and  $c_3$  (right) considering all the oil viscosities for all the displacements for the front shock absorber.

If you look at the first graphs, you can see that the fact that there are errors in the force signal at low viscosities is reflected in the coefficients, which are not correct at all for 0.5 mm and 1 mm displacement.

Regarding the coefficient  $c_1$ , it can be seen that it increases, starting from a certain value greater than zero, as the viscosity of the oil increases. On the contrary, the coefficient  $c_3$  decreases from a certain negative value, except for the displacements of 2.5 mm and 3mm, where we have already seen previously that for low viscosities  $c_3$  is positive with a low absolute value around zero.

## 7. 3D maps of the damping coefficients

The dependence of coefficient  $c_1$  and coefficient  $c_3$  on displacement and viscosity can be combined in two 3D graph, with a graduated colour scale to see the difference in values, as shown in Figure 7.1 for  $c_1$ , Figure 7.2 for  $c_3$ .

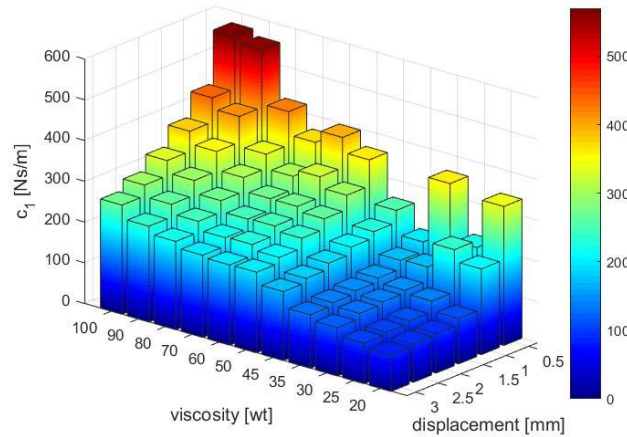


Figure 7.1 – 3D map of the damping coefficient  $c_1$  for the different displacements and viscosities.

Seeing the first map, the coefficient  $c_1$  increases if the viscosity increases and if the displacement decreases with some errors at low displacements.

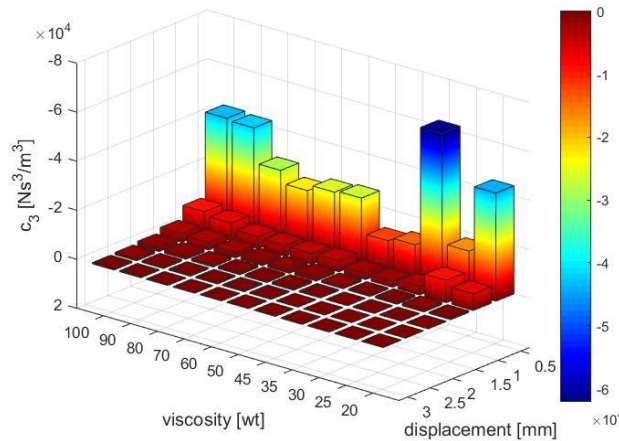


Figure 7.2 – 3D map of the damping coefficient  $c_3$  for the different displacements and viscosities.

From this graph, the trend of the coefficients on the two parameters is not very clear, as they differ even by an order of magnitude if the displacement is increased.

In Figure 7.3 there is a magnification of Figure 7.2 that considers only the displacements 1.5 mm, 2 mm, 2.5 mm, 3 mm, because otherwise it can't really be seen the difference.

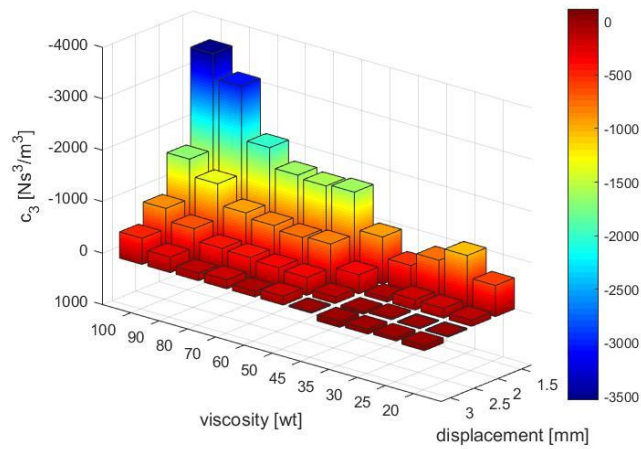


Figure 7.3 – Magnification of the 3D map of the damping coefficient  $c_3$  for the different viscosities and displacements 1.5 mm, 2 mm, 2.5 mm, 3 mm.

Looking at the trend of  $c_3$  it also increases, in absolute value because it is negative in almost all cases, by increasing the viscosity and decreasing the displacement. For low viscosities and high displacement in some cases there are also positive values of  $c_3$  or near zero.

## Conclusions

The aim of this thesis was to analyze the experimental measurements and data concerning shock absorbers for a vehicle in 1:5 scale, and to create a damping model that considers these data, identifying a damping characteristic. The analysis of the experimental data shows that, unless some experimental errors, the front and rear shock absorbers show the same results for the damping force. However, there are some test sets with results that deviate from the others, such as cases where the viscosity is low, and the piston stroke is too small and clean signals cannot be obtained.

After analysing the experimental data, to find the damping coefficient for each test it was necessary to interpolate the damping force by trying a series of regression forms. Finally, looking at the results, the cubic polynomial with only odd terms was chosen. After understanding the best form of regression, the trend of the two damping coefficients  $c_1$  and  $c_3$  on the imposed displacement and viscosity were analysed by considering all the tests. From the analysis the first increases with increasing oil viscosity and decreasing imposed displacement, while the second one, being negative in most cases, increases in absolute value as the viscosity increases and the displacement decreases.

## Reference

- [1] De Giuseppe G., *Experimental setup for RC car suspensions*, MSc Thesis, I Facoltà di Ingegneria Politecnico di Torino, 2019.
- [2] [https://en.wikipedia.org/wiki/Shock\\_absorber](https://en.wikipedia.org/wiki/Shock_absorber) available in 2021-11-28.
- [3] <https://racenrcs.com/rc-cars-and-shock-oil-explained> available in 2021-11-28.